The Effect of Motion on Joint Estimates of Activity and Attenuation from Time-of-Flight PET Data

Ahmadreza Rezaei[1], Johan Nuyts[1], and Michel Defrise[2]

***Abstract*— Recent studies show that joint reconstruction of activity and attenuation is possible with time-of-flight PET data. However, when there is motion during the acquisition of the emission data, the properties of the reconstructions are not known. In this study, we classify three theoretical types of motion and analyze joint reconstructions when the emission data has been affected by each type separately. We use the existing TOF-MLAA algorithm for this purpose and observed that motion during the scan can make the data inconsistent, such that the resulting reconstructions are not only affected by motion blur, but also suffer from artifacts.**

I. Introduction

It is known that motion in PET and PET/CT can result in errors due to incorrect attenuation correction in addition to motion blur in the estimated emission image [1]. In [2], it was shown that a difference in emission and transmission resolution can also introduce artifacts due to attenuation correction of the emission data. Different methods have been proposed to correct the emission data affected by motion during the scan when gated data are not available [3]–[5]. In gated PET studies however, it is preferable to acquire a single CT scan, register the attenuation images non-rigidly to the PET images before attenuation correction and correct for attenuation in the data using the deformed (registered) CT scans for each phase in the cardiac/respiratory cycle [6]–[8]. Recent studies have shown that when time-of-flight (TOF) data are available, joint reconstruction of the activity and attenuation is possible up to a scale factor [9]–[11]. Hamill and Panin [5] have shown that when motion occurs during the PET-scan, MLAA produces a blurred mu-map, yielding better attenuation correction than is obtained from a fast, motion-free CT scan. However, the exact effect of motion during acquisition on the joint reconstruction of activity and attenuation is not clearly known. In order to further investigate the effects of motion, we identify different types of motion that theoretically could occur during the emission measurements, simulate each type and analyze the final activity and attenuation reconstructions. We use the existing algorithm for maximum likelihood estimation of activity and attenuation (MLAA) [10] and compare the reconstructed images to reference ML images. The reference activity image is produced with MLEM (maximum likelihood expectation maximization) assuming that the attenuation is known, and the reference attenuation image is computed with MLTR (maximum likelihood for transmission tomography) assuming knowledge about the true tracer distribution. Our main result is that TOF-MLAA produces consistent pairs of activity and attenuation reconstructions that best describe the emission data when the motion either affects the activity or the attenuation (first 2 motion types), but not both. Our simulations indicate that in the case of simultaneous motion in activity and attenuation (type 3 motion), the emission data are no longer consistent, i.e. there exists no value for the estimated parameters (here the activity and the attenuation) that would produce the measured data, using the current acquisition model (the model here assumes a motion free object). Thus, TOF-MLAA can only reconstruct the consistent portion of the emission data. Nevertheless, we see that the region which is not affected by the motion can be quantitatively reconstructed. In the case of inconsistencies in the emission sinogram, it is not known whether the emission measurements could be split into multiple consistent emission measurements or if it is possible to retrieve information about the motion by analyzing the emission measurements.

[1] Dept. of Nuclear Medicine, Katholieke Universiteit Leuven, B-3000, Leuven, Belgium, [2]Dept. of Nuclear Medicine, Vrije Universiteit Brussel, B-1090 Brussels, Belgium. E-mails: ahmadreza.rezaei@uz.kuleuven.be, johan.nuyts@uz.kuleuven.be, and mdefrise@vub.ac.be

[3]This research is supported by a research grant (GOA) from K.U.Leuven.

II. Methods

In order to have a better understanding of the effect of motion in the joint estimation problem, we analyze three types of motion, i.e. 1- motion in the activity image, 2- motion in the attenuation image and 3- simultaneous motion in both the activity and attenuation images. Although the first two types of motion may not be as common as the third type (type 2 motion in particular seems rather unrealistic), the analysis gives additional insight into the problem of motion in joint image reconstruction. We will simulate the motion in successive frames, make projections of each frame and sum over all projections. We then attempt to reconstruct the motion affected measurements and compare the results with the total activity (summed over all frames) and average attenuation (average over all frames).

We model the TOF-PET expected counts $\bar{y}_{it} = a_i p_{it}$ for line of response (LOR) i and TOF-bin t as the multiplication of the (unattenuated) TOF projections of the activity image p_{it} and the attenuation factors a_i which are computed as

$$p_{it} = \sum_{j=1}^{J} c_{ijt}\lambda_j, \quad a_i = e^{-\sum_{j=1}^{J} l_{ij}\mu_j} \tag{1}$$

where λ_j and μ_j are the activity and attenuation coefficient at voxel j, J is the total number of voxels, c_{ijt} is the sensitivity of the measurement bin at (i,t) for activity in j in absence of attenuation and l_{ij} is the intersection length of LOR i with voxel j.

A. Activity Motion

The measurements due to this type of motion can be expressed as,

$$\bar{y}_{it} = \sum_{f=1}^{F} \bar{y}_{it}^{f} = a_i \sum_{f=1}^{F} p_{it}^{f} \tag{2}$$

where the superscript f determines the time frame and F is the total number of time frames.

In this type of motion, the attenuation image remains stationary over all time frames Thus reconstructing the measurements $\bar{y}_{it}$, we expect to obtain the stationary attenuation image together with the total activity image.

B. Attenuation Motion

The measurements due to this type of motion can be expressed as,

$$\bar{y}_{it} = \sum_{f=1}^{F} \bar{y}_{it}^{f} = F p_{it} \sum_{f=1}^{F} \frac{a_i^f}{F} \tag{3}$$

In this type of motion, the activity is stationary. Reconstructing the measurements $\bar{y}_{it}$, we expect to obtain F times the stationary activity image together with some "equivalent" attenuation image. Some attenuation correction methods use the average of CT scans extrapolated to the required photon energy of 511 keV. However, it can be seen from eq (3) that the time averaging happens over the attenuation factors, and not over the attenuation images [6].

C. Activity and Attenuation Motion

In this type of motion, since neither the activity image nor the attenuation images are stationary, the measurements $\bar{y}_{it}$ can not be expressed in any simpler form. We define the "residual error" (TOF) sinogram as the difference between the measured data y_{it} and the expected data $\bar{y}_{it}$ corresponding to the forward projection of the activity and attenuation reconstructions. These residuals were very different from zero, indicating that the measurements y_{it} affected by this motion are no longer consistent under a motion-free reconstruction model.

III. Experimental Design and Results

Just to keep things simple, we simulated the activity and attenuation images in three different time frames (F=3), figure 1. A disk-like object was moved within the object to simulate the three types of motions discussed. The disk-like object was set to the background value to simulate the stationary attenuation and activity phantoms in the first two types of motion.

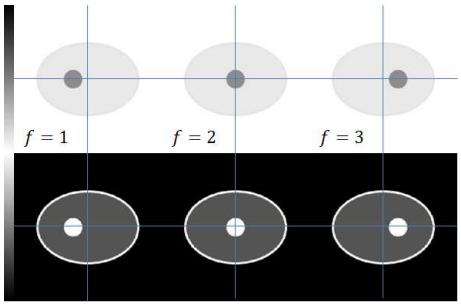

Fig. 1. Activity (top) and attenuation (bottom) images at three different frames (left, center and right) used in the study.

For the simulations below, 2D TOF emission data were generated and organized in 200 radial bins, 168 azimuthal angles, 13 TOF-bins of 312 ps width and with an effective TOF resolution of 580 ps. An oversampling of 3 (i.e. 3 rays per LOR, 9 sub-pixels per image pixel) was used during the simulation, to avoid an exact match between the simulation and the (back)projection during reconstruction. The activity and attenuation images were then reconstructed in a 200×200 pixel grid with a pixel size of 4.1×4.1 mm^2. Activity and attenuation reconstructed using MLAA are then compared to activity reconstructions of MLEM with known attenuation and to attenuation reconstructions of MLTR with known activity, respectively. The MLAA reconstructions are after 3 iterations of 28 subsets, cycling over the attenuation image 5 times for each update of the emission image [10]. The reconstructions of MLEM are after 3 iterations of 28 subsets and the reconstructions of MLTR are after 15 iterations of 28 subsets.

A. Activity Motion - Type I

Since the attenuation image is stationary in this type of motion, the exact attenuation image was projected and used for attenuation correction of the reference MLEM emission reconstruction. We also used the sum of all the activity images as a blank scan to reconstruct the reference attenuation image using the MLTR algorithm. Figure 2 shows horizontal profiles through the center of the reconstructed activity and attenuation images from MLTR, MLEM and MLAA.

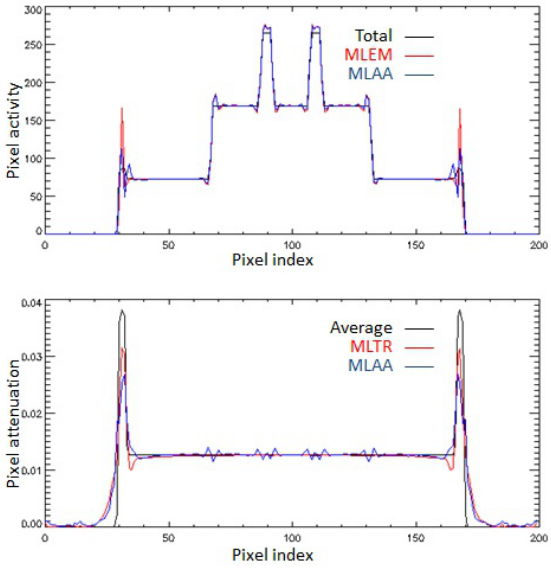

Fig. 2. Horizontal activity (top) and attenuation (bottom) profiles through the MLTR, MLEM and MLAA reconstructions affected by the type I motion. The ML activity and attenuation profiles are compared to the total activity and the average attenuation image of the different time frames, respectively.

The profiles reveal a close agreement between the MLAA reconstructions and the ML reference images. As expected, it can be seen that motion of the activity during the scan results in smoothness (motion blur) of the reconstructed activity image.

B. Attenuation Motion - Type II

In the type II motion, the activity image is stationary. Hence, we use its projections (multiplied by F) as a blank scan to reconstruct the reference attenuation image using MLTR. To simulate the approach where the resolution of the attenuation and activity are matched, we use the projections of the average attenuation image as the corresponding attenuation

that needs to be accounted for during MLEM reconstructions of the activity. Figure 3 shows similar profiles through MLTR, MLEM and MLAA reconstructions of attenuation and activity.

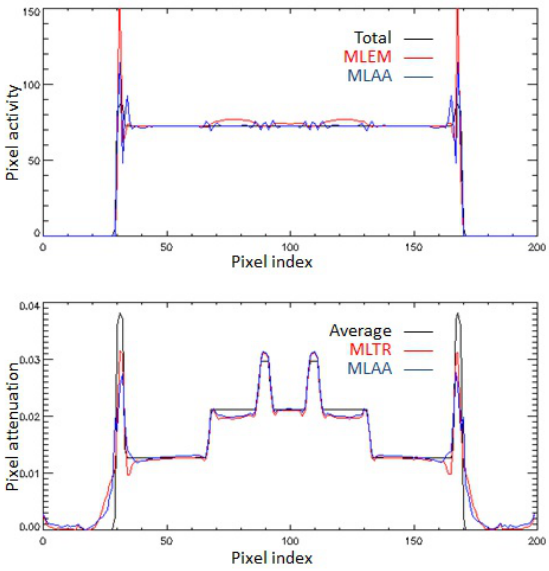

Fig. 3. Horizontal activity (top) and attenuation (bottom) profiles through the MLEM, MLTR and MLAA reconstructions affected by the type II motion.

It can be seen that given the total activity images over multiple frames, MLTR produces an attenuation that is different from the average attenuation. Interestingly, we see that MLAA has been able to produce an attenuation profile similar to the one of MLTR. We will refer to this as an "equivalent" attenuation image, which corresponds to the attenuation image best describing the attenuation correction factors averaged over the time frames as in eq (3) (as opposed to an average over the attenuation images). The difference seen between the average attenuation image and the equivalent attenuation image is due to the nonlinearity of the exponential law of Beer-Lambert.

Figure 3 also shows that the activity profile that was produced using MLEM and the average attenuation image suffers from artifactual increase of the tracer activity in the region which has been affected by this type of motion. In contrast, MLAA was able to produce activity and attenuation images that are better consistent with the emission measurements.

C. Activity and Attenuation Motion - Type III

In this type of motion, neither the activity nor the attenuation images are stationary. However, we will still use the projections of the total activity (which we optimistically would like to recover) to reconstruct an attenuation image with MLTR and use the average attenuation image, as before, to reconstruct the activity image with MLEM. Figure 4 shows the two horizontal profiles of the reconstructed activity and attenuation images from MLTR, MLEM and MLAA.

The activity profiles of figure 4 show that neither MLAA nor MLEM with knowledge of the average attenuation image accurately estimate the total tracer distribution image. Furthermore, MLAA and MLTR with knowledge of the total activity produced different horizontal attenuation profiles. We have also tried reconstructing the total activity using MLEM with the "equivalent" attenuation image, however the result differed

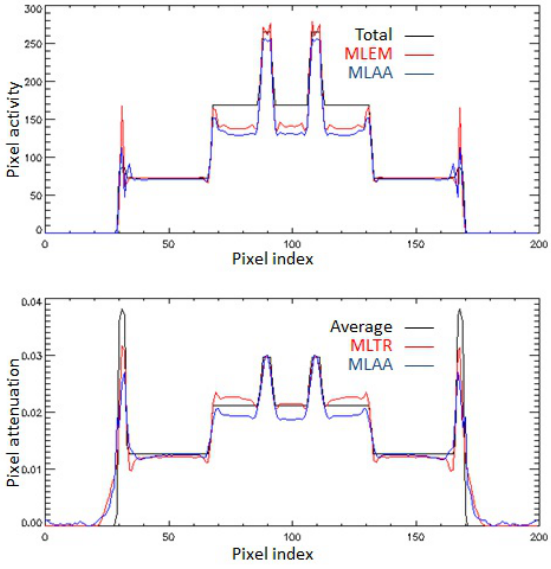

Fig. 4. Horizontal activity (top) and attenuation (bottom) profiles through the MLEM, MLTR and MLAA reconstructions affected by the type III motion.

significantly from the true total activity and was also slightly different from the MLAA activity (profile not shown here).

D. Inconsistencies Due to Motion

The residual error sinograms were calculated for the three motion cases, and we observed signs of inconsistencies in the case of the type III motion. Figure 5 shows (non-TOF) sinograms of the mean and variance, computed by averaging the residual error sinograms over the 13 TOF-bins.

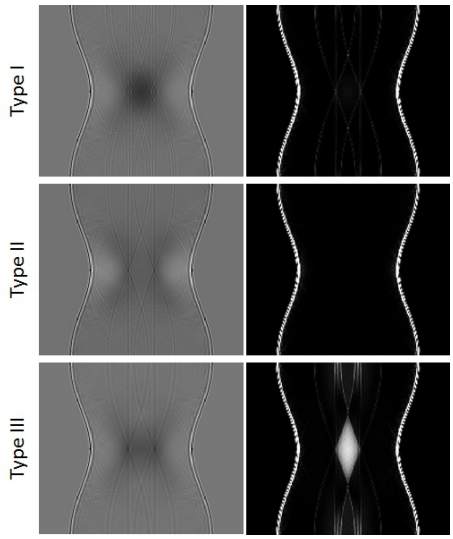

Fig. 5. Mean (left) and variance (right) over the TOF-bins of the residual error sinogram for the type I (top), type II (middle) and type III (bottom) motions. The grey scale is identical for all images.

Figure 5 shows that when there is motion in the activity and attenuation images (type III motion), the mean TOF-bin error does not show significant signs of inconsistencies. However, the variance image shows that in some LORs, there are fairly large positive and negative errors, indicating that for this type of motion the emission data are no longer consistent. We believe that this is why MLAA has not been able to accurately estimate the total activity image in the type III motion.

Fig 5 also shows that the residuals are much larger near the boundary of the sinogram. This is because these LORs have a short intersection with the object, and therefore have few counts, and provide only very limited information. This issue is better described in [9].

E. Locality of the Motion-Affected Region

In the case of the type III motion, we analyzed the image region that is affected. The same phantom of figure 1 was used with the addition of extra details to the phantom. MLAA activity and attenuation reconstructions after 10 iterations and 28 subsets were compared to the total activity and average attenuation, respectively.

Figure 6 shows the reference images, the MLAA reconstructions and the absolute value of the differences between both. The difference images were multiplied with 10 and displayed with the same intensity window as the corresponding reconstructions.

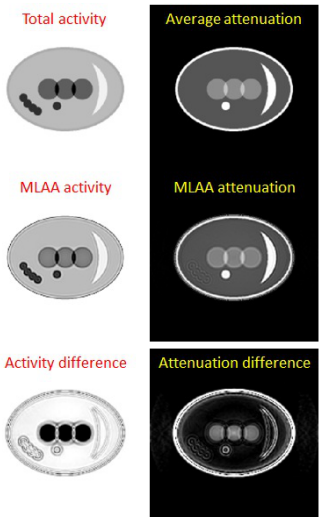

Fig. 6. Reference (top), reconstructed (middle) and ten times the error (bottom) between the activity (left) and attenuation (right) images affected by type III motion. The three images in each column are displayed with the same intensity window.

Figure 6 shows that motion affected the reconstructions locally, while the regions not affected by motion were reconstructed with a good quantitative accuracy.

IV. Discussion and Conclusion

TOF-PET data determine the attenuation sinogram up to a constant [9], and joint estimation of attenuation and activity with a maximum likelihood algorithm was found to be successful and surprisingly stable [10]. In clinical PET/CT imaging, often attenuation correction artifacts are observed, which are due to a geometric mismatch between CT and PET. This mismatch can be caused by patient motion between the CT and PET scans and by motion during the PET scan. The joint estimation of attenuation and emission from the same scan data obviously eliminates between-scan motion. Joint estimation is also assumed to provide an ”optimal” reconstruction in the case of in-scan motion, where ”optimal” means that the solution maximizes the likelihood. However, it was not clear to what extent this ”optimal” activity reconstruction would correspond to the best image that one can hope to obtain from a single ungated scan with motion, which is a motion blurred version of the true activity image.

In this work, we classify motion in the measurements into three types of motion, activity motion, attenuation motion and simultaneous activity and attenuation motion. In the first two types of motion, it was observed that MLAA was able to reconstruct a pair of activity and attenuation images that agreed (almost) exactly with the emission data. The MLAA activity and attenuation images are quantitatively close to MLEM reconstructions of activity with known attenuation and MLTR reconstructions of attenuation with known activity. In the case of type II motion, it was also shown that using the projections of the average attenuation images can result in motion errors in the reconstructed activity image.

In the case of type III motion, the MLAA activity and attenuation profiles were significantly different from the activity reconstruction of MLEM and the attenuation reconstruction of MLTR in the motion affected regions of the reconstructions. Apparently, in this case the emission data are no longer consistent and MLAA has been able to reconstruct only the consistent parts of the emission data. The inconsistency of the data affected by the type III motion is suggested by large values in the TOF residuals sinogram. In our simulations, it appears that LORs which intersect the moving object the most, happen to be the ones that see a high variance in the residual error sinogram. Further investigation is required to check whether or not is it possible to split an inconsistent sinogram into multiple consistent ones or to retrieve information about the motion by analyzing the inconsistencies in the residual errors.

References

[1] M Osman, C Cohade, Y Nakamoto, R Wahl, “Respiratory motion artifacts on PET emission images obtained using CT attenuation correction on PET-CT”, *Eur J Nucl Med Mol Imaging.*, 2003, 30(4):603-606.

[2] A Chatziioannou, M Dahlborn, “Detailed investigation of transmission and emission data smoothing protocols and their effects on emission images”, *IEEE Trans. Nucl. Sci.*, 1996, 43(1):290-294.

[3] T Pan, O Mawlawi, S Nehmeh, *et al.*, “Attenuation Correction of PET Images with Respiration-Averaged CT Images in PET/CT”, *J Nucl Med*, 2005, 46(9):1481-1487.

[4] R Cook, G Carnes, T Lee, G Wells, “Respiration-Averaged CT for Attenuation Correction in Canine Cardiac PET/CT”, *J Nucl Med*, 2007, 48(5):811-818.

[5] J Hamill, V Panin, “TOF-MLAA for Attenuation Correction in Thoracic PET/CT”, *2012 IEEE Nuclear Science Symposium and Medical Imaging Conference, Anaheim*, 2012, paper M23-1.

[6] J Hamill, G Bosmans, A Dekker, “Respiratory-gated CT as a tool for the simulation of breathing artifacts in PET and PET/CT”, *Med Phys*, 2008, 35(2):576-585.

[7] M Dawood, F Buther, X Jiang, K Schafers, “Respiratory Motion Correction in 3-D PET Data With Advanced Optical Flow Algorithms”, *IEEE Trans. Med. Imag.*, 2008, 27(8):1164-1175.

[8] S McQuade, T Lambrou, B Hutton, “A novel method for incorporating respiratory-matched attenuation correction in the motion correction of cardiac PETCT studies”, *Phys. Med. Biol.*, 2011, **56**:2903-2915.

[9] M Defrise, A Rezaei, J Nuyts, “Time-of-flight PET data determine the attenuation sinogram up to a constant”, *Phys. Med. Biol.*, 2012, **57**:885-899.

[10] A Rezaei, M Defrise, G Bal, C Michel, M Conti, C Watson, J Nuyts, “Simultaneous reconstruction of activity and attenuation in Time-of-flight PET”, *IEEE Trans. Med. Imag.*, 2012, 31(12):2224-2233.

[11] J Nuyts, A Rezaei, M Defrise, “ML-reconstruction for TOF-PET with simultaneous estimation of the attenuation factors”, *2012 IEEE Nuclear Science Symposium and Medical Imaging Conference, Anaheim*, 2012, paper M04-1.